Lipid Bilayer Electrostatic Energy, Curvature Stress, and Assembly of Gramicidin Channels†

Jens A. Lundbæk,*,‡ Andreia M. Maer, and Olaf S. Andersen*

Department of Physiology and Biophysics, Cornell University Medical College, New York, New York 10021

Received August 7, 1996; Revised Manuscript Received February 10, 1997⊗

ABSTRACT: Hydrophobic interactions between lipid bilayers and imbedded membrane proteins couple protein conformation to the mechanical properties of the bilayer. This coupling is widely assumed to account for the regulation of membrane protein function by the membrane lipids' propensity to form nonbilayer phases, which will produce a curvature stress in the bilayer. Nevertheless, there is only limited experimental evidence for an effect of bilayer curvature stress on membrane protein structure. We show that alterations in curvature stress, due to alterations in the electrostatic energy of dioleoylphosphatidylserine bilayers, modulate the structurally well-defined gramicidin A monomer ↔ dimer reaction. Maneuvers that decrease the electrostatic energy of the unperturbed bilayer promote channel dissociation; we measure the change in interaction energy. The bilayer electrostatic energy thus can affect membrane protein structure by a mechanism that does not involve the electrostatic field across the bilayer, but rather electrostatic interactions among the phospholipid head groups in each monolayer which affect the bilayer curvature stress. These results provide further evidence for the importance of mechanical interactions between a bilayer and its imbedded proteins for protein structure and function.

In a lipid bilayer the equilibrium curvature of the monolayers will depend on the balance of the intermolecular forces among the lipid head groups relative to those among the acyl chains (Kirk et al., 1984; Seddon, 1990). The equilibrium monolayer curvature may be positive as in micelles, zero, or negative as in H_{II} phases (Figure 1A). Biological membranes contain large amounts of lipids that in isolation form nonbilayer structures; the bilayers therefore exist in a state of curvature stress, where the tendency of each monolayer to adopt a nonplanar conformation is opposed by hydrophobic interactions between the monolayers [e.g., Seddon (1990)]. The control of protein function by the phase preference of the membrane lipids [e.g., Navarro et al. (1984), Hui and Sen (1989), Seddon (1990), Keller et al. (1993), Brown (1994), McCallum and Epand (1995), and Chang et al. (1995)] may arise because of hydrophobic coupling between integral membrane proteins and the surrounding bilayer (Mouritsen & Bloom, 1984). These hydrophobic interactions will couple the protein conformational preference to changes in bilayer curvature stress (Gruner, 1991; Epand & Epand, 1994) and, more generally, the bilayer deformation energy (Andersen et al., 1992; Lundbæk & Andersen, 1994).

In contrast to the many examples of protein *function* being altered by maneuvers that alter bilayer curvature stress, there is a paucity of experimental studies that directly probe how curvature stress affects protein *conformation* (Gruner, 1991). Keller et al. (1993) examined the equilibrium distribution among different conducting states of alamethicin channels in planar bilayers formed by a mixture of DOPC and DOPE: an increase in the mole fraction of DOPE, which increases the H_{II} phase propensity, shifts the distribution of conductance levels toward the higher conductance levels. Brown (1994) examined how the equilibrium distribution between metarhodopsin-I and metarhodopsin-II in the photocycle of mammalian rhodopsin varies as a function of phospholipid head group size, as well as acyl chain length, unsaturation, and branching: changes in bilayer lipid composition that increase the H_{II} phase propensity shift the equilibrium toward metarhodopsin-II. In either case, however, there is only limited information about the protein structures that are affected by the bilayer curvature stress.

It therefore becomes important to have quantitative measurements that probe how (maneuvers that affect) the bilayer curvature stress affects structurally well-defined membrane proteins (Gruner, 1991). In the present study, we use gA[1] channels in DOPS/*n*-decane bilayers to probe how protein conformation can be coupled to bilayer curvature stress. gA channels are miniproteins that form membrane-spanning ion channels in lipid bilayers. The channels are dimers (Bamberg & Läuger, 1973; Veatch et al., 1975; Cifu et al., 1992) formed by the transmembrane dimerization of two nonconducting monomers (O'Connell et al., 1990) that are inserted into each monolayer as $\beta^{6.3}$-helices (Figure 1B) (He et al., 1994); see Koeppe and Andersen (1996) for a recent review. The channels' hydrophobic exterior, ∼2.2 nm (Elliott et al., 1983), is shorter than the average hydrophobic thickness of the bilayer, ∼5 nm for *n*-decane-containing bilayers (Benz & Janko, 1976). gA channel formation therefore involves a compression and bending of the monolayers toward each other.

†Supported in part by NIH Grant GM21342 (O.S.A.), by a grant from the Danish Medical Research Council (J.A.L.), and by a predoctoral fellowship from NSF (A.M.M.).

* To whom correspondence should be sent.

‡ Present address: Department of Neuropharmacology, Novo-Nordisk A/S, Novo-Nordisk Park, DK-2760 Måløv, Denmark.

⊗ Abstract published in *Advance ACS Abstracts,* April 15, 1997.

[1] Abbreviations: gA, gramicidin A; DOPC, dioleoylphosphatidylcholine; DOPE, dioleoylphosphatidylethanolamine; DOPS, dioleoylphosphatidylserine; HEPES, *N*-(2-hydroxyethyl)piperazine-*N*′-2-ethanesulfonic acid; EDTA, ethylenediaminetetraacetic acid; TEA^+, tetraethylammonium; $[Na^+]_i$, and $[Ca^{2+}]_i$, interfacial $[Na^+]$ and $[Ca^{2+}]$.

S0006-2960(96)01984-8 CCC: $14.00

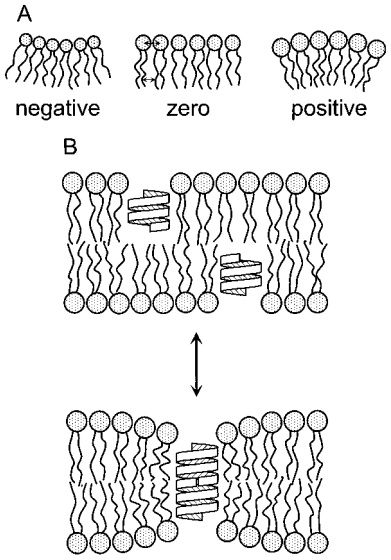

FIGURE 1: (A) Depending on the balance of the intermolecular forces among the lipid head groups relative to those among the acyl chains (indicated by arrows), the equilibrium curvature of a lipid monolayer may be positive (as in micelles), zero, or negative (as in H_{II} phases) (Kirk et al., 1984; Seddon, 1990). (B) Gramicidin channels form by the transmembrane association of a monomer from each monolayer. This causes a local increase in curvature stress. Channel dissociation causes a corresponding decrease in stress.

In lipid monolayers, the variation in intermolecular lateral interactions along the molecular axis, which determines the equilibrium curvature, usually is expressed as an effective "shape" of the molecules in the monolayer (Tartar, 1955; Israelachvili et al., 1976; Cullis & deKruijff, 1979) (Figure 1A). Molecules that have a cylindrical "shape" form planar monolayers with zero equilibrium curvature; if the effective cross-sectional area at the polar head group region is larger than that of the acyl chains, the monolayer will have a positive equilibrium curvature; if the effective cross-sectional area is less than that of the acyl chains, the monolayer will have a negative curvature. The equilibrium curvature can be altered pharmacologically, by the addition of amphipathic molecules that differ in the cross-sectional areas of the polar head group and of the acyl chain(s) or by physicochemical means, e.g., by altering lipid head group hydration or charge or by increasing the temperature, which increases the effective acyl chain area (Cullis & deKruijff, 1979; Seddon, 1990; Tate et al., 1991). Whatever the underlying mechanism, a change in monolayer curvature will alter the molecular packing in both the head group and acyl chain regions [cf. Kirk et al. (1984)].

In the present experiments, the electrostatic repulsion among the negatively charged phosphatidylserine head groups in DOPS bilayers was decreased by increases in $[H^+]$, $[Ca^{2+}]$, $[Mg^{2+}]$, and ionic strength. The diminished electrostatic repulsion produces a negative monolayer equilibrium curvature (Kirk et al., 1984; Bezrukov et al., 1995; R. P. Rand, personal communication), which will produce a bilayer curvature stress and increase the H_{II} phase propensity [e.g., Tate et al. (1991)].[2] In bilayers where the monolayers have a negative equilibrium curvature, gA channel formation will further increase the curvature stress in the immediately surrounding bilayer; the energetic cost associated with this increase in stress will vary with the magnitude of the curvature stress in the unperturbed bilayer (C. Nielsen, M. Goulian, and O. S. Andersen, manuscript in preparation). Channel dissociation will release the increased stress. One would thus expect that experimental maneuvers that decrease the electrostatic repulsion among the phosphatidylserine head groups will decrease gA channel stability and average duration. As we show in this article, that turns out to be the case.

[2] In DOPS bilayers, H_{II} phase formation is seen only at high $[H^+]$; H_{II} structures are not observed at high $[Ca^{2+}]$ or [NaCl] (Coorssen & Rand, 1995; R. P. Rand, personal communication).

METHODS AND MATERIALS

Single-channel measurements were done using the bilayer punch (Andersen, 1983). The current signal was amplified using an AxoPatch 1B instrument (Axon Instruments, Foster City, CA). Stock solutions of HPLC-purified gA (a gift from R. E. Koeppe, II, University of Arkansas) (1−10 nM) were made up in ethanol and added to the electrolyte solution at nominal concentrations between 1 pM (at low $[Ca^{2+}]$) and 20 pM (at high $[Ca^{2+}]$). DOPS was from Avanti Polar Lipids Inc. (Alabaster, AL) and used without further purification. Except when specifically noted, the bilayer-forming solution was DOPS in *n*-decane (2−3% w/v) using *n*-decane (99.9% pure) from Wiley Organics (Columbus, OH). Unless otherwise noted, the electrolyte solution was 0.1 M NaCl (EM Science, Cherry Hill, NJ), 5 mM HEPES (Sigma Chemical Co., St. Louis, MO), pH 7. Other buffers used were phosphate and glycylglycine (Sigma). The electrolyte solution was made up daily using Milli-Q water (Millipore Corp., Bedford, MA). $[Ca^{2+}]$ was increased by the addition of $CaCl_2$ (EM Science) to the electrolyte solution. In the absence of added Ca^{2+}, $[Ca^{2+}]$ was ∼1 μM (measured fluorometrically). In the presence of 100 μM EDTA (Sigma), $[Ca^{2+}]$ was ∼0.5 nM. All experiments were done at 25 ± 1 °C.

In the single-channel experiments, the current signal was filtered at 50−100 Hz and digitized and sampled by a PC/AT compatible computer; transitions were detected on-line (Andersen, 1983). The membrane potential was 200 mV. Single-channel average durations were determined by fitting single exponential distributions, $N(t) = N(0) \exp(-t/\tau)$, where τ is the average channel duration, $N(0)$ the total number of channels, and $N(t)$ the number of channels with a duration longer than t, to the duration distributions (Durkin et al., 1990).

The effect of Ca^{2+} on gA channel activity in DOPS bilayers was determined in separate experiments in which the conductance of gA containing planar bilayers (∼1.6 mm^2) was measured using a membrane potential of 5−20 mV (filtered at 0.1 Hz). The electrolyte solution was stirred throughout the experiments. The specific capacitance of DOPS/*n*-decane bilayers was measured using a sawtooth potential across planar bilayers.

RESULTS

Increases in $[Ca^{2+}]$ have profound effects on gA channels in DOPS bilayers (Figure 2), as both the single-channel conductance and τ decrease when $[Ca^{2+}]$ is increased. The effect is concentration dependent with the major effects occurring >1 μM. At 1 mM Ca^{2+}, τ is 7-fold less than in the nominal absence of Ca^{2+} (Figures 3 and 4).

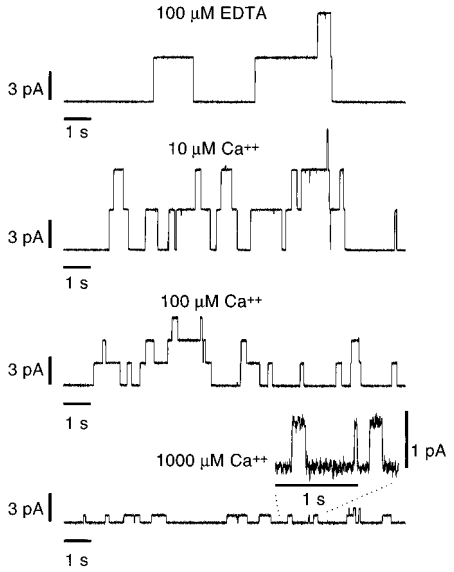

FIGURE 2: Single-channel current traces showing the effect of Ca^{2+} on gA channels in DOPS/*n*-decane bilayers.

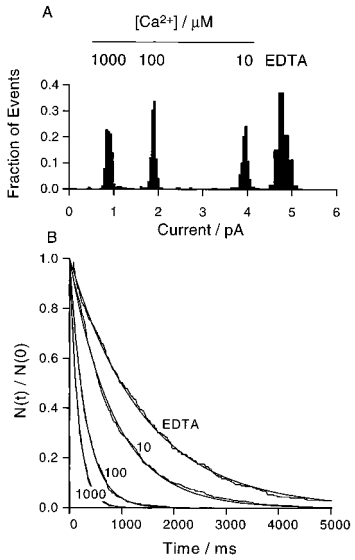

FIGURE 3: (A) Current transition amplitude histograms for gA channels in DOPS/*n*-decane bilayer. (B) Normalized survivor histograms for gA channels; the labels 10, 100, and 1000 refer to $[Ca^{2+}]$ in μM, and the label EDTA refers to an experiment with 100 μM EDTA. In both the (nominal) absence and presence of Ca^{2+} the single channel distribution histograms can be described by single exponential distributions.

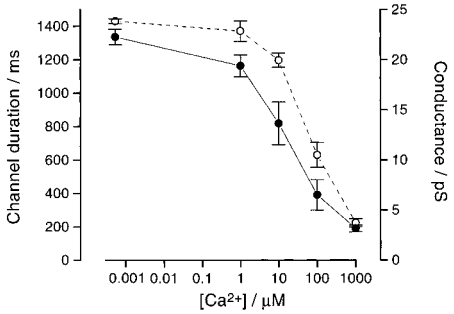

FIGURE 4: Effect of Ca^{2+} on the average duration (●, solid line, left ordinate) and conductance of gA channels (○, interrupted line, right ordinate). Each point represents mean ± SE, $n \geq 3$.

In agreement with earlier findings (Gambale et al., 1987), the single-channel conductance is decreased when $[Ca^{2+}]$ is increased (Figures 2−4). Examination of the current transition amplitude (Figure 3A) and duration (Figure 3B) histograms shows that there is a single population of gA channels at all $[Ca^{2+}]$ used in this study. By visual inspection, the bilayers appeared to be homogeneous and fluid, and their electrical conductance was not affected by the Ca^{2+} addition indicating that Ca^{2+} did not induce the formation of nonbilayer structures (which is expected to increase the bilayer conductance). We conclude there is no evidence for a Ca^{2+}-induced phase transition (or phase separation) in the bilayer.

Table 1: Effect of pH, $[Ca^{2+}]$, $[Mg^{2+}]$, Ionic Strength, and Lipid Composition on the gA Channel Duration and Specific Capacitance of Bilayers

	τ (ms) ± SE	specific capacitance (μF/cm^2) ± SE
DOPS/*n*-decane[a]		
0.1 M Na^+, pH 7 (HEPES)	1340 ± 50	0.379 ± 0.007
0.1 M Na^+, pH 7 (phosphate)	1320 ± 70	
0.5 M Na^+, pH 7 (HEPES)	1040 ± 50	
1.0 M Na^+, pH 7 (HEPES)	680 ± 50	
0.1 M Na^+, pH 7, 0.001 M $Ca2^+$ (HEPES)	190 ± 20	0.390 ± 0.010
0.1 M Na^+, pH 7, 0.001 M Mg^{2+} (HEPES)	500 ± 20	
0.1 M Na^+, pH 3 (glycylglycine)	170 ± 10	
0.1 M Na^+, pH 3 (phosphate)	230 ± 20	
0.15 M Na^+, 0.35 M TEA^+, pH 7 (HEPES)	1390 ± 190	
DOPE/DOPS (2:1)/*n*-decane		
0.1 M Na^+, pH 7 (HEPES)	140 ± 20	
DOPC/DOPS (2:1)/*n*-decane		
0.1 M Na^+, pH 7 (HEPES)	470 ± 50	
DOPC/*n*-decane[b]		
0.75 M Na^+	380 ± 30	
0.75 M Na^+, 0.05 M Ca^{2+}	460 ± 10	

[a] In experiments with DOPS, DOPE/DOPS (2:1), or DOPC/DOPS (2:1), 100 μM EDTA was added to all experiments done in the nominal absence of Ca^{2+}. [b] The electrolyte compositions in the DOPC experiments were chosen to conform with the DOPS experiments, where $[Na^+]_i$ and $[Ca^{2+}]_i$ in 0.1 M NaCl plus 1 mM Ca^{2+} at pH 7 are ~0.75 and ~0.05 M, respectively.

Mg^{2+} is less potent than Ca^{2+}: 1 mM Mg^{2+} causes only an approximately 3-fold reduction in τ (Table 1), most likely because DOPS' affinity for Mg^{2+} is less than its Ca^{2+} affinity (McLaughlin et al., 1981). An increase in $[H^+]$ also has a qualitatively similar effect as an increase in $[Ca^{2+}]$: lowering the pH from 7 to 3 decreases τ 7-fold (Table 1). The decrease in τ does not result from a change in bilayer thickness because the specific membrane capacitance is unaffected by the addition of Ca^{2+} (Table 1).

Fraley et al. (1980) reported that Ca^{2+}-induced fusion of phosphatidylserine vesicles varied with the buffer used, which could suggest that ion induced changes in bilayer curvature stress were dependent on the choice of buffer. The effects of Ca^{2+} or H^+ on gA channels, however, are not dependent on the specific choice of buffer. HEPES is one of the good buffers; it does not bind Ca^{2+} (Good et al., 1966). At pH 7 (0.1 M NaCl), the average single-channel conductance and duration are the same in HEPES or phosphate buffers (Table 1); at pH 3 (0.1 M NaCl), the average single-channel conductance and duration are similar in glycylglycine or phosphate buffers (Table 1) (conductance results not shown).

H^+, Ca^{2+}, and Mg^{2+} bind to phosphatidylserine bilayers (Papahadjopoulos, 1968; McLaughlin et al., 1981) and

decrease the magnitude of the surface charge density. In addition, the divalent Ca^{2+} will screen any negative surface charge (McLaughlin et al., 1971). (The increase in $[H^+]$ is too small to exert a significant screening effect.) An increase in either $[Ca^{2+}]$ or $[H^+]$ therefore will decrease the magnitude of the surface potential, and thus $[Na^+]_i$, of DOPS bilayers. But the decrease in τ does not result from a decreased $[Na^+]_i$ *per se*: When $[Na^+]$ is decreased from 0.5 to 0.15 M at a constant ionic strength, using tetraethylammonium (TEA^+) as inert electrolyte, τ is not decreased (Table 1). Further, when the ionic strength is increased by increasing $[Na^+]$ from 0.1 to 1.0 M NaCl, which has minimal effect on $[Na^+]_i$, τ is decreased 2-fold (Table 1).

The surface charge density also was altered by replacing some of the DOPS by either DOPE or DOPC (0.1 M NaCl, pH 7). In either case, there was a several-fold reduction in τ (Table 1). The reduction was largest in DOPE/DOPS bilayers, most likely because the polar head group volume is larger for DOPC than for DOPE [e.g., Lundbæk and Andersen (1994)]. The single-channel conductances were similar, ~15 pS (results not shown), indicating that the surface charge densities are comparable in these bilayers. Finally, in uncharged DOPC/*n*-decane bilayers, Ca^{2+} does not decrease the channel stability (Table 1), which indicates that the reduction in τ does not result from specific interactions between Ca^{2+} and gA channels.

The effect of Ca^{2+} on gA channel activity, the number of membrane-spanning conducting dimers (*D*), was determined by measuring the Ca^{2+}-induced changes in the conductance of gA containing DOPS bilayers (Figure 5).

When $[Ca^{2+}]$ was increased from (nominally) 0 to 100 μM, the overall membrane conductance due to gA channels decreased by a factor of 130 (experiment in Figure 5A). The change in channel activity is calculated as

$$D_{Ca}/D_{cntrl} \approx [(G_{Ca} - G_b)/(G_{cntrl} - G_b)]/(g_{Ca}/g_{cntrl}) \quad (1)$$

where the subscripts cntrl and Ca denote the absence and presence of Ca^{2+}. G is the aggregate conductance of the channels plus bilayer, G_b the background bilayer conductance, and g the single-channel conductance. The decrease in membrane conductance when Ca^{2+} was increased from 0 to 100 μM corresponds to a 60-fold reduction in channel activity; subsequent removal of Ca^{2+} (by chelating with EDTA) increased the conductance toward its value before Ca^{2+} addition (Figure 5). Increases in $[H^+]$ and ionic strength had similar effects on channel activity, as judged by the need to increase the aqueous gA concentrations in order to get a channel appearance rate of 1 s^{-1} in single-channel experiments where the pH was lowered or the ionic strength was increased (results not shown).

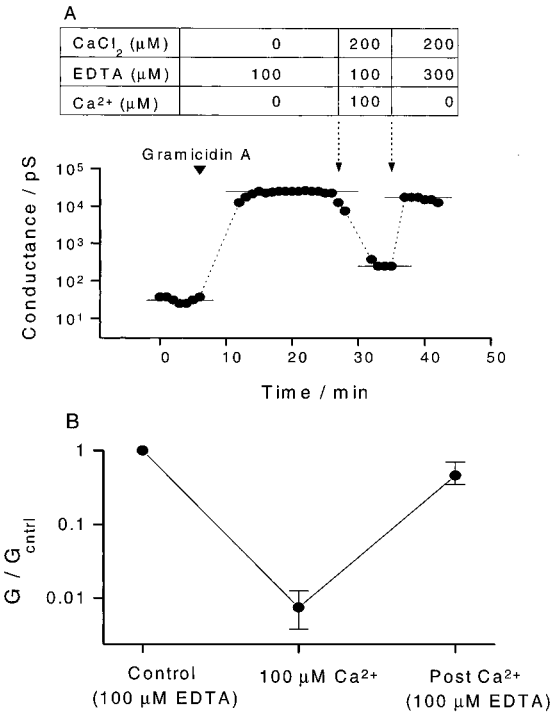

FIGURE 5: Effect of 100 μM Ca^{2+} on gA channel activity in a DOPS/*n*-decane bilayer. (A) Results from a single experiment where the gA-induced changes in the conductance of a bilayer were determined. The conductance was initially measured in nominally Ca^{2+} free solutions (0.1 M NaCl, 100 μM EDTA, 5 mM HEPES, pH 7). First arrow, when gA (~1 pM) was added to the electrolyte solution bathing the bilayer the conductance rose to a stable level (indicated by the stable line) over ~10 min. Second arrow, addition of 200 μM $CaCl_2$ to both solutions ($[Ca^{2+}] = 100$ μM) decreased the conductance to a new steady level over ~6 min. Third arrow, addition of 200 μM EDTA ($Ca^{2+} = 0$ μM) increased the conductance to a new level over ~2 min. The solutions were stirred continuously. (B) Summary of the effect of 100 μM Ca^{2+} on the gA-induced conductance (G) of DOPS/*n*-decane bilayers. Each point represents the geometric mean ± range of G/G_{cntrl} ($n = 3$).

DISCUSSION

We have shown that increases in $[Ca^{2+}]$, $[Mg^{2+}]$, $[H^+]$, and ionic strength decrease the stability and average duration of gA channels in DOPS bilayers. These changes in channel behavior are in qualitative agreement with predictions based on changes in bilayer curvature stress due to decreased repulsion among the head groups. Moreover, it is possible to calculate the change in the free energy of dimerization and relate this to the change in electrostatic energy per DOPS (see below). Before doing so, however, we need to discuss several possible concerns.

(1) The experimental maneuvers used here increase the H_{II} phase propensity of DOPS bilayers (Tate et al., 1991).[2] H_{II} phases did not form, however. If a H_{II} phase had formed, the bilayer would be physically disrupted or lose its electrical barrier properties, which was not observed. In 1 mM Ca^{2+}, the bilayers remained stable, the bilayer conductance was unchanged; moreover, the visual appearance of the bilayers appeared normal, and the specific capacitance (the bilayer thickness) was unchanged. These observations indicate that liquid-crystalline bilayer structure was maintained.

(2) In mixed phosphatidylserine/phosphatidylcholine bilayers, addition of Ca^{2+} can induce lateral phase separations (Ohnishi & Ito, 1974; Haverstick & Glaser, 1987). When DOPS is the only lipid component, such lateral phase separation should not occur, and no signs of phase separations were observed in the experiments either by visually inspecting the bilayers or in the behavior of gA channels. In phase-separated bilayers, for example, gA channel formation in the different phases induces a heterogeneous channel behavior (Knoll et al., 1986). In our experiments, the channels constituted a homogeneous population in terms of both current transition amplitude and duration distributions (Figure 3).

(3) The present experiments were done using *n*-decane-containing bilayers. That should not affect our conclusion that the changes in gA channel stability arise from a change

in the material properties of the bilayer (see below). Kirk and Gruner (1985) showed that the presence of a hydrocarbon filler does not affect the qualitative phase behavior of H_{II}-forming phospholipids, but rather relieves hydrocarbon packing constraints such that the intrinsic monolayer curvature becomes better expressed. Moreover, 1 mM Ca^{2+} does not affect the bilayer thickness, which indicates that the acyl chain packing is relatively unaffected by the Ca^{2+} addition.[3] The thickness of the nonpolar core of *n*-decane-containing phospholipid bilayers is approximately twice that of nominally hydrocarbon-free bilayers [cf. Benz et al. (1975) and Benz and Janko (1976)], indicating that 50% of the core volume is *n*-decane. *n*-Decane-containing bilayers have a thickness that is twice that of a fully extended acyl chain, ~0.13 nm/CH_2 group [cf. Tartar (1955) and McIntosh et al. (1980)]. When a gA channel forms, *n*-decane therefore will be "squeezed" out of the bilayer as the acyl chains are compressed. The thickness of hydrocarbon-free DOPC bilayers is ~2.6 nm (Benz et al., 1975; Lewis & Engelman, 1983), about 0.4 nm more than the hydrophobic exterior length of a gA channel. In close proximity to a gA channel, there will be little if any *n*-decane, and the acyl chain packing will approximate that in a hydrocarbon-free bilayer.

(4) The decreased gA channel stability is not due to specific ion−channel interactions. First, gA has no titratable groups, gA channels do not bind Ca^{2+} with high affinity (Urry et al., 1982), and Ca^{2+} does not decrease the channel stability in uncharged DOPC/*n*-decane bilayers (the slight increase in τ in 50 mM Ca^{2+} is insignificant in comparison with the DOPS results). Second, the decreased channel duration does not result from a decrease in $[Na^+]_i$ due to a Ca^{2+}- or H^+-induced decrease in the magnitude of the surface potential. τ is *decreased* when $[Na^+]$ is *increased* from 0.1 to 1.0 M NaCl (Table 1), and there is no decrease in τ when $[Na^+]$ is decreased at a constant ionic strength (Table 1).

On the basis of the above arguments, we conclude that the decreased gA channel stability and duration are due to altered lipid bilayer−channel interactions. Given that there are no specific interactions between gramicidin channels and their host bilayer (Providence et al., 1995), we further conclude that the gA channel is affected by the material properties of the lipid bilayer. The changes in the electrostatic repulsion among the phospholipid head groups caused by increases in $[Ca^{2+}]$, $[Mg^{2+}]$, $[H^+]$, and ionic strength will alter the lipid packing in a manner that can be summarized as changes in monolayer equilibrium curvature. These changes in curvature will lead to a change in the curvature stress in the bilayer (Kirk et al., 1984),[4] which leads to an increased bilayer deformation energy associated with gA channel formation.

The effect of curvature stress on the energetics of gA dimerization can be calculated from the changes in channel activity. The equilibrium between monomers (M) and dimeric channels (D) is described by

$$K = [D]/[M]^2 \quad (2)$$

where K is the dimerization constant. At low gA concentrations, when $[M] \gg [D]$, which is the case here, K is proportional to [D] [e.g., Lundbæk and Andersen (1994)]. The free energy of dimerization therefore is

$$\Delta\Delta G^\circ = -RT \ln(K_{Ca}/K_{cntrl}) \approx -RT \ln([D]_{Ca}/[D]_{cntrl}) \quad (3)$$

where the subscripts cntrl and Ca denote the absence and presence of Ca^{2+}, R is the gas constant, and T is the temperature in Kelvin. Figure 6 shows the changes in K and $\Delta\Delta G^\circ$ caused by the addition of 100 μM Ca^{2+} (the experiments from Figure 5); K decreased by a factor of 60 and $\Delta\Delta G^\circ$ increased by 10 kJ/mol (of gA channels).

For comparison, the changes in the electrostatic free energy (ΔG°_{el}) of a DOPS bilayer was estimated using Gouy−Chapman−Stern theory [e.g., McLaughlin (1982)]. Addition of 100 μM Ca^{2+} (in 0.1 M NaCl) changes ΔG°_{el} by ~0.2 kT/DOPS molecule (1 kJ/mol). A $\Delta\Delta G^\circ$ of +10 kJ/mol (Figure 6) thus corresponds to the change in the electrostatic energy of the 20 lipid molecules in the annulus immediately surrounding the gramicidin channel (10 in each monolayer). It is in this context important that our experimental maneuvers alter not only the electrostatic repulsion among the phospholipid head groups but also nonelectrostatic contributions to the head group packing, such as bulk and hydration (Portis et al., 1979). The importance of these nonelectrostatic contributions is illustrated by the different durations in DOPE/DOPS and DOPC/DOPS bilayers (Table 1).

When the Ca^{2+}-induced changes in K are decomposed into the changes in dimerization and dissociation rate constants (k_1 and k_{-1}, respectively), k_1 is decreased ~20-fold whereas k_{-1} is increased only 3-fold (Figure 6). This asymmetry is expected; it arises because gA channel formation causes a large bilayer deformation, involving a change in bilayer thickness from ~5 nm in the unperturbed bilayer to ~2.2 nm adjacent to the channel. Channel dissociation, in contrast, occurs when the gA monomers move only ~0.16 nm apart [e.g., Durkin et al. (1993) and Lundbæk et al. (1996)].

At present, the regulation of protein function by the host bilayer remains poorly understood. Our results provide additional insights into how hydrophobic interactions between a lipid bilayer and embedded proteins allow the mechanical properties of the bilayer to modulate protein function. Generally, maneuvers that produce a negative monolayer equilibrium curvature (that increase the H_{II} phase propensity) *decrease* gA channel stability: changes in head group size (Neher & Eibl, 1977; Maer et al., 1997); long-chain alcohols (Pope et al., 1982); cholesterol, (Pope et al., 1982; Lundbæk et al., 1996); present results. Conversely, micelle-forming compounds *increase* gA channel stability (Sawyer et al., 1989; Sawyer & Andersen, 1989; Lundbæk & Andersen, 1994; Lundbæk et al., 1996). Importantly, all the above results can be rationalized simply by considering the average "shape" of the molecules in the bilayer and the associated curvature stress.

It is in this context important that alamethicin channels respond to similar experimental manipulations as gA channels (Keller et al., 1993; Bezrukov et al., 1995). Maneuvers that promote the dimerization of gA channels reduce the probability of observing the higher conductance levels in alamethicin channels (cf. Neher and Eibl (1977) and Keller

[3] Wilschut et al. (1980) showed that the Ca^{2+}-induced fusion of unilamellar phosphatidylserine vesicles occurs at a "threshold concentration" of 1−2 mM. The Ca^{2+}−phosphatidylserine interactions that underlie vesicle fusion differ from those in bilayers (Portis et al., 1979; Feigenson, 1986), as Ca^{2+} forms a 1:2 Ca^{2+}−phosphatidylserine complex that forms *between* the vesicles (with one phosphatidylserine molecule coming from each vesicle).

[4] The importance of electrostatic interactions among the polar head groups for lipid packing was emphasized by Tartar (1955).

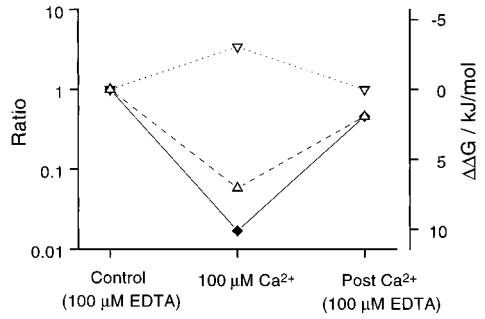

FIGURE 6: Effect of 100 μM Ca^{2+} on the kinetics and energetics of gA channel formation. Left ordinate, effect of 100 μM Ca^{2+} on K (◆), k_1 (△), and k_{-1} (▽). The changes in k_1 and k_{-1} were calculated as $k_{-1}/k_{-1,cntrl} = \tau_{cntrl}/\tau$ and $k_1/k_{1,cntrl} = (K_{cntrl}/K)(k_{-1}/k_{-1,cntrl})$. Right ordinate, the corresponding changes in the free energy of dimerization and the activation energies for channel association and dissociation.

et al. (1993)]; maneuvers that reduce the dimerization of gA channels enhance the probability of observing the higher conductance states in alamethicin channels (Bezrukov et al., 1995; present study).

This ability to alter the function of membrane-spanning channels by altering the properties of the surrounding bilayer has biological significance, when integral membrane proteins undergo conformational changes that involve the protein/lipid interface [e.g., Unwin and Ennis (1984) and Unwin et al. (1988)]. Not surprisingly, therefore, manipulations that alter the monolayer curvature produce predictable changes in membrane protein structure and function. This is illustrated by the results of Brown (1994) on the metarhodopsin-I ↔ metarhodopsin-II equilibrium. There is no information about length changes of the membrane-spanning rhodopsin domain; but the metarhodopsin-I → metarhodopsin-II transition is associated with a 0.4 nm increase in average membrane thickness (Salamon et al., 1994), and conformations with an increased hydrophobic length should be stabilized by maneuvers that increase the H_{II}-forming propensity of the membrane lipids. Indeed, the equilibrium distribution is shifted toward metarhodopsin-II when the H_{II}-propensity of the host bilayer is increased (Brown, 1994). Changes in bilayer curvature stress appear to constitute a general mechanism for modulating membrane protein conformation and function, due to the contribution of the bilayer deformation energy to the free energy cost of protein conformational changes.

ACKNOWLEDGMENT

We thank Randi B. Silver for assistance with the fluorometric [Ca^{2+}] determination, Lyndon L. Providence for assistance with some of the bilayer experiments, and Mark Goulian, Roger E. Koeppe II, Claus Nielsen, and R. Peter Rand for helpful discussions and comments on the manuscript.

REFERENCES

Andersen, O. S. (1983) *Biophys. J. 41*, 119−133.

Andersen, O. S., Sawyer, D. B., & Koeppe, R. E., II (1992) in *Biomembrane Structure and Function* (Gaber, B. P., & Easwaran, K. R. K., Eds.) pp 227−244, Adenine Press, Schenectady, NY.

Bamberg, E., & Läuger, P. (1973) *J. Membr. Biol. 11*, 177−194.

Benz, R., & Janko, K. (1976) *Biochim. Biophys. Acta 455*, 721−738.

Benz, R., Fröhlich, O., Läuger, P., & Montal, M. (1975) *Biochim. Biophys. Acta 394*, 323−334.

Bezrukov, S. M., Vodyanoy, I., Rand, P., & Parsegian, V. A. (1995) *Biophys. J. 68*, A341.

Brown, M. F. (1994) *Chem. Phys. Lipids 73*, 159−180.

Chang, H. M., Reitstetter, R., Mason, R. P., & Gruener, R. (1995) *J. Membr. Biol. 143*, 51−63.

Cifu, A. S., Koeppe, R. E., II, & Andersen, O. S. (1992) *Biophys. J. 61*, 189−203.

Coorssen, J. R., & Rand, R. P. (1995) *Biophys. J. 68*, 1009−1018.

Cullis, P. R., & de Kruijff, B. (1979) *Biochim. Biophys. Acta 559*, 399−420.

Durkin, J. T., Koeppe, R. E., II, & Andersen, O. S. (1990) *J. Mol. Biol. 211*, 221−234.

Durkin, J. T., Providence, L. L., Koeppe, R. E., II, & Andersen, O. S. (1993) *J. Mol. Biol. 231*, 1102−1121.

Elliott, J. R., Needham, D., Dilger, J. P., & Haydon, D. A. (1983) *Biochim. Biophys. Acta 735*, 95−103.

Epand, R. M., & Epand, R. F. (1994) *Biophys. J. 66*, 1450−1456.

Feigenson, G. W. (1986) *Biochemistry 25*, 5819−5825.

Fraley, R., Wilschut, J., Duzgunes, N., Smith, C., & Papahadjopoulos, D. (1980) *Biochemistry 19*, 6021−6029.

Gambale, F., Menini, A, & Rauch, G. (1987) *Eur. Biophys. J. 14*, 369−374.

Good, N. E., Winget, G. D., Winter, W., Connolly, T. N., Izawa, S., & Singh, R. M. M. (1966) *Biochemistry 5*, 467−477.

Gruner, S. M. (1991) in *Biologically Inspired Physics* (Peliti, L., Ed.) pp 127−135, Plenum Press, New York.

Haverstick, D. M., & Glaser, M. (1987) *Proc. Natl. Acad. Sci. U.S.A. 84*, 4475−4479.

He, K., Ludtke, S. J., Wu, Y., Huang, H. W., Andersen, O. S., Greathouse, D., & Koeppe, R. E., II (1994) *Biophys. Chem. 49*, 83−89.

Hui, S.-W., & Sen, A. (1989) *Proc. Natl. Acad. Sci. U.S.A. 86*, 5825−5829.

Israelachvili, J. N., Mitchell, D. J., & Ninham, B. W. (1976) *J. Chem. Soc., Faraday Trans. 2 72*, 1525−1568.

Keller, S. L., Bezrukov, S. M., Gruner, S. M., Tate, M. W., Vodyanoy, I., & Parsegian, V. A. (1993) *Biophys. J. 65*, 23−27.

Kirk, G. L., & Gruner, S. M. (1985) *J. Phys. (Paris) 46*, 761−769.

Kirk, G. L., Gruner, S. M., & Stein, D. L. (1984) *Biochemistry 23*, 1093−1102.

Knoll, W., Apell, H. J., Eibl, H., & Miller, A. (1986) *Eur. Biophys. J. 13*, 187−193.

Koeppe, R. E., II, & Andersen, O. S. (1996) *Annu. Rev. Biophys. Biomol. Struct. 25*, 231−258.

Lewis, B. A., & Engelman, D. M. (1983) *J. Mol. Biol. 166*, 211−217.

Lundbæk, J. A., & Andersen, O. S. (1994) *J. Gen. Physiol. 104*, 645−673.

Lundbæk, J. A., Birn, P., Girshman, J., Hansen, A. J., & Andersen, O. S. (1996) *Biochemistry 35*, 3825−3830.

Maer, A. M., Providence, L. L., & Andersen, O. S. (1997) *Biophys. J. 72*, A191, abstract.

McCallum, C. D., & Epand, R. M. (1995) *Biochemistry 34*, 1815−1824.

McIntosh, T. J., Simon, S. A., & MacDonald, R. C. (1980) *Biochim. Biophys. Acta 597*, 445−463.

McLaughlin, S. (1982) in *Membranes and Transport* (Martonosi, A., Ed.) pp 51−55, Plenum Press, New York.

McLaughlin, S. G. A., Szabo, G., & Eisenman, G. (1971) *J. Gen. Physiol. 58*, 667−687.

McLaughlin, S., Mulrine, N., Gresalfi, T., Vaio, G., & McLaughlin, A. (1981) *J. Gen. Physiol. 77*, 445−473.

Mouritsen, O. G., & Bloom, M. (1984) *Biophys. J. 46*, 141−153.

Navarro, J., Toivio-Kinnucan, M., & Racker, E. (1984) *Biochemistry 23*, 130−135.

Neher, E., & Eibl, H. (1977) *Biochim. Biophys. Acta 464*, 37−44.

O'Connell, A. M., Koeppe, R. E., II, & Andersen, O. S. (1990) *Science 250*, 1256−1259.

Ohnishi, S., & Ito, T. (1974) *Biochemistry 13*, 881−887.

Papahadjopoulos, D. (1968) *Biochim. Biophys. Acta 163*, 240−254.

Pope, C. G., Urban, B. W., & Haydon, D. A. (1982) *Biochim. Biophys. Acta 688*, 279−283.

Portis, A., Newton, C., Pangborn, W., & Papahadjopoulos, D. (1979) *Biochemistry 18*, 780−790.
Providence, L. L., Andersen, O. S., Greathouse, D. V., Koeppe, R. E., II, & Bittman, R. (1995) *Biochemistry 34*, 16404−16411.
Salamon, Z., Wang, Y., Brown, M. F., Macleod, H. A., & Tollin, G. (1994) *Biochemistry 33*, 13706−13711.
Sawyer, D. B., & Andersen, O. S. (1989) *Biochim. Biophys. Acta 987*, 129−132.
Sawyer, D. B., Koeppe, R. E., II, & Andersen, O. S. (1989) *Biochemistry 28*, 6571−6583.
Seddon, J. M. (1990) *Biochim. Biophys. Acta 1031*, 1−69.
Tartar, H. V. (1955) *J. Phys. Chem. 59*, 1195−1199.
Tate, M. W., Eikenberry, E. F., Turner, D. C., Shyamsunder, E., & Gruner, S. M. (1991) *Chem. Phys. Lipids 57*, 147−164.
Unwin, N., Toyoshima, C., & Kubalek, E. (1988) *J. Cell. Biol. 107*, 1123−1138.
Unwin, P. N. T., & Ennis, P. D. (1984) *Nature 307*, 609−613.
Urry, D. W., Trapane, T. L., Walker, J. T., & Prasad, K. U. (1982) *J. Biol. Chem. 257*, 6659−6661.
Veatch, W. R., Mathies, R., Eisenberg, M., & Stryer, L. (1975) *J. Mol. Biol. 99*, 75−92.
Wilschut, J., Düzgünes, N., Fraley, R., & Papahadjopoulos, D. (1980) *Biochemistry 19*, 6011−6021.

BI9619841